

# Effects of mean curvature on flame propagation

I. Ahmed and N. Swaminathan

Department of Engineering, University of Cambridge, Cambridge, CB2 1PZ

## 1 Introduction

The initial flame kernels of spark-ignition engines and accidental or controlled explosions are some examples of where one could find outwardly propagating spherical flames. Often the studies of such spherical flames use the results obtained from statistically planar flames, where the mean curvature effects are absent. Direct Numerical Simulation (DNS) studies [1, 2] have shown that the curvature induces significant effects on the propagation of flame fronts and flame brushes. It is expected that any change in the local strain or curvature (collectively called as stretch) would impart due influence on the scalar gradient. Thus, a parameter related to the scalar gradient would be an appropriate choice to capture these effects on turbulent flame propagation.

In this work, the Reynolds-Averaged Navier Stokes (RANS) methodology will be used to study the propagation of premixed turbulent spherical flames. The reaction rate is modelled using a recently developed strained flamelet model [3]. The mean scalar dissipation rate of a progress variable is used to parametrise the strained flamelet and it is defined as  $\bar{\rho}\tilde{\epsilon}_c = \overline{\rho\alpha(\nabla c'' \cdot \nabla c'')}$ , where  $c''$  is the Favre fluctuation of a progress variable  $c$  with molecular diffusivity  $\alpha$ . The progress variable is defined in terms of temperature  $T$  as  $c = (T - T_u)/(T_b - T_u)$ , with the subscripts  $b$  and  $u$  respectively denoting the burnt and unburnt mixture. The mean scalar dissipation rate is obtained from an algebraic model described later. The aim of this work is to determine the effects of mean curvature on the propagation speed of turbulent flames. This is achieved by simulating turbulent spherical flames using reaction rate models accounting for mean curvature effects through the scalar dissipation rate.

## 2 Reaction rate model

In this work the reaction rate is modelled using the recently developed strained flamelet model of Kolla & Swaminathan [3], which gives the mean reaction rate as:

$$\bar{\omega} = \int_0^1 \left[ \int_0^{N_{\max}} \dot{\omega}(\zeta, \psi) P(\psi|\zeta) d\psi \right] P(\zeta) d\zeta, \quad (1)$$

where  $\zeta$  and  $\psi$  are the sample space variables respectively for  $c$  and  $N$ ,  $P(\zeta)$  is the probability density function (pdf) of  $c$  and  $P(\psi|\zeta)$  is the conditional pdf. Here the presumed pdf approach is used to define these two pdfs. A  $\beta$  pdf is used for  $P(\zeta)$  and a log-normal pdf is used for the conditional dissipation rate pdf as discussed in [3].

The Favre mean progress variable  $\tilde{c}$  and its variance  $\tilde{c}''^2$ , required for the  $\beta$  pdf are obtained by solving their transport equations. As discussed in [3], the mean dissipation rate required for the log-normal pdf is obtained using

$$\tilde{\epsilon}_c = \frac{1}{\beta'} \left[ (2K_c^* - \tau C_4) \frac{s_L^0}{\delta_L^0} + C_3 \frac{\tilde{\epsilon}}{k} \right] \tilde{c}''^2, \quad (2)$$

where the heat release parameter  $\tau$  is defined as  $\tau \equiv (T_b - T_u)/T_u$ ,  $s_L^0$  and  $\delta_L^0$  are respectively the unstrained laminar flame speed and thermal thickness. The Favre-averaged turbulent kinetic energy and its dissipation rate are respectively denoted by  $\tilde{k}$  and  $\tilde{\varepsilon}$ . The model parameters are:  $\beta' = 6.7$ ,  $K_c^* = 0.85\tau$  for hydrocarbon-air mixtures,  $C_3 = 1.5\sqrt{Ka}/(1 + \sqrt{Ka})$  and  $C_4 = 1.1/(1 + Ka)^{0.4}$ . The Karlovitz number  $Ka$  is defined by,  $Ka \equiv \sqrt{(u'/s_L^0)^3(\delta/\Lambda)}$ , where  $\delta_L^0 = \delta[2(1 + \tau)^{0.7}]$ ,  $u' = \sqrt{2\tilde{k}/3}$  and  $\Lambda = u'^3/\tilde{\varepsilon}$ . The flamelet reaction rate is obtained using opposed flow laminar premixed flames in reactant-to-product (RtP) configuration following [3].

The dissipation rate model in Eq. (2) was developed for planar flames [5] with high Reynolds and Damköhler numbers and thus it only includes strain effects. The effects of mean curvature on the scalar dissipation rate  $\tilde{\varepsilon}_c$  are captured as follows: the transport equation for  $\tilde{\varepsilon}_c$  has been studied in [6] to address the influence of mean curvature on the evolution of  $\tilde{\varepsilon}_c$  and the modelling of various terms in its transport equation. These results are used to obtain an algebraic model, which includes the mean curvature effects by balancing the leading order terms in the  $\tilde{\varepsilon}_c$  transport equation when the Reynolds and Damköhler numbers are large. This model is written as:

$$\tilde{\varepsilon}_c \simeq \frac{1}{\beta'} \left\{ \left[ 2K_c^* - \tau C_4 \left( 1 - \frac{\alpha_u}{s_L^0} \nabla \cdot \mathbf{n} \right) \right] \frac{s_L^0}{\delta_L^0} + C_3^* \Gamma_K \frac{\tilde{\varepsilon}}{\tilde{k}} \right\} \tilde{c}''^2, \quad (3)$$

where the normal vector is defined as  $\mathbf{n} = -\nabla \tilde{c}/|\nabla \tilde{c}|$ , the model constant  $C_3^* = 3$  and  $\Gamma_K$  is an efficiency function proposed by Meneveau & Poinso [7] to account for the reduced turbulent straining when the flame radius is small [6]. This term is of order of unity. It is clear from Eqs. (2) and (3) that the main difference between these two model is the curvature effects arising from  $\nabla \cdot \mathbf{n}$  term, which is zero for statistically planar flames. The model in Eq. (3) is *unconditionally realisable* for exploding flames but for imploding flames the realisability criteria imposes a minimum radius for which the model will be valid.

### 3 RANS calculations of spherical flames

The outwardly-propagating spherical flames are computed using the RANS methodology. Spherical symmetry is assumed, hence, only the radial dependence is retained. The computer code used in [3], which solves the mass and momentum conservation equations along with the  $k - \varepsilon$  modelled equations, is modified for spherical co-ordinates. The thermochemistry is tracked using balance equations for  $\tilde{c}$  and  $\tilde{c}''^2$  and state equation. The reaction rate is closed using Eq. (1) and the dissipation rate is modelled using Eq. (2) or (3) to exclude or include the mean curvature effects. The reactive source terms in  $\tilde{c}''^2$  equation is closed in a consistent manner.

Although a spherically symmetric flame is considered, it is worth to write the  $r$ -momentum and turbulent kinetic energy equation to bring out additional effects which are present in spherical systems. The  $r$ -momentum equation for high turbulent Reynolds number flow is:

$$\frac{\partial \tilde{\rho} \tilde{u}_r}{\partial t} + \frac{1}{r^2} \frac{\partial}{\partial r} [r^2 (\tilde{\rho} \tilde{u}_r^2)] = -\frac{\partial \tilde{p}}{\partial r} - \frac{1}{r^2} \frac{\partial}{\partial r} \left[ r^2 (\overline{\rho u_r''^2}) \right] + \frac{(\overline{\rho u_\theta''^2} + \overline{\rho u_\phi''^2})}{r}, \quad (4)$$

and turbulent kinetic energy equation is:

$$\begin{aligned} \frac{\partial \tilde{\rho} \tilde{k}}{\partial t} + \frac{1}{r^2} \frac{\partial}{\partial r} [r^2 (\tilde{\rho} \tilde{u}_r \tilde{k})] &= \frac{1}{r^2} \frac{\partial}{\partial r} \left\{ r^2 \left[ \left( \mu + \frac{\mu_t}{Sc_k} \right) \frac{\partial \tilde{k}}{\partial r} \right] \right\} - \frac{2}{3} \left( \frac{\partial \tilde{u}_r}{\partial r} + 2 \frac{\tilde{u}_r}{r} \right) \tilde{\rho} \tilde{k} \\ &+ \frac{4}{3} \mu_t \left( \frac{\partial \tilde{u}_r}{\partial r} - \frac{\tilde{u}_r}{r} \right)^2 - \tilde{\rho} \tilde{\varepsilon} + \overline{u_r'} \frac{\partial \tilde{p}}{\partial r} + \overline{p' \nabla \cdot \mathbf{u}''}, \end{aligned} \quad (5)$$

where  $\mu$  and  $\mu_t$  represent the molecular and turbulent viscosities, respectively. The centrifugal forces  $\overline{\rho u_\theta''^2}/r$  and  $\overline{\rho u_\phi''^2}/r$  arise from the turbulent Reynolds stresses. Due to the three-dimensional nature

of turbulence these Reynolds stress terms do not vanish even for the case of a spherically symmetric problem. Since these terms are divided by the radius  $r$  it is expected that these additional source terms will be significant in the initial period of flame development and will slowly disappear as the flame radius increases. Note that since the  $k - \varepsilon$  model is used in this work the Reynolds stress terms are closed using the Boussinesq approximation, which implies that the terms  $\overline{\rho u''_\theta{}^2}$  and  $\overline{\rho u''_\phi{}^2}$  are identical. However, if an anisotropic turbulence model is used these Reynolds stresses will be different.

The second and third terms appearing on the RHS of the above modelled kinetic energy equation are a result of writing the unclosed production term  $-\overline{\rho(\mathbf{u}'' \otimes \mathbf{u}'')} : \nabla \tilde{u}$  in spherical coordinates and closing the Reynolds stress terms using Boussinesq approximation. Here again, the term  $\tilde{u}_r/r$  is due to the spherical coordinate system. The last two terms on the RHS of Eq. (5) represent the pressure work and pressure dilatation terms respectively. These terms are often ignored in turbulent flame calculations. The pressure dilatation is closed using  $0.5\tilde{c}(\tau s_L^0)^2 \bar{\omega}$  and the Reynolds-averaged fluctuating velocity appearing in the pressure work term is obtained using  $\overline{u''} = \widetilde{u_r'' c''} \times \tau / (1 + \tau \tilde{c})$ . The scalar flux is modelled as a gradient flux.

### 3.1 Simulation parameters

As mentioned in § 2, RtP flamelet configuration is used in this work. The mean reaction rate  $\bar{\omega}$  required for RANS calculation is calculated from these flamelets *a priori*, using GRI-3.0 chemical kinetics mechanism for methane-air flames. These calculated reaction rates are tabulated as a function of  $\tilde{c}$ ,  $\tilde{c}''^2$  and  $\tilde{\varepsilon}_c$  and a trilinear interpolation is used to obtain  $\bar{\omega}$  during the RANS calculations, for the values of  $\tilde{c}$ ,  $\tilde{c}''^2$  and  $\tilde{\varepsilon}_c$ .

The stoichiometric methane-air flames at 298 K and atmospheric pressure are considered. The thermochemical characteristics of this flame are:  $s_L^0 = 0.4$  m/s,  $\delta_L^0 = 0.41$  mm and  $\tau = 6.48$ . The characteristics of the turbulent flames calculated numerically are given in Table 1. The stretch factor  $K$  given in this table is defined by  $K = 0.157(u'/s_L^0)^2/\sqrt{\text{Re}_t}$  where the turbulent Reynolds number is defined as  $\text{Re}_t \equiv (u'\Lambda)/\nu_u$ , with  $\nu_u$  denoting the kinematic viscosity of the fresh gases and the Damköhler number is defined as  $\text{Da} = (s_L^0/u')(\Lambda/\delta)$ . The flames F1 and F2 have  $K = 1$  and they are in the thin reaction zones regime. The flame F1 has  $K = 0.15$  and is in the corrugated flamelets regime.

The domain length required for RANS simulations varies from 0.25 m to 1.0 m and the grid spacing varies from 0.083 mm to 0.33 mm. These values are dictated by the turbulent flame conditions. Uniform grid spacing is used with at least 10 grid points inside  $\min(\Lambda, \delta_t)$  for a given turbulence condition. The turbulent flame brush thickness is given by  $\delta_t \equiv 1/|\partial\tilde{c}/\partial r|_{\text{max}}$ . The size of the time step is chosen to be 0.1  $\mu\text{s}$  for all flames simulated for this study. Initial values of  $\tilde{k}$  and  $\tilde{\varepsilon}$  for the fresh gases are specified for the entire computational domain. An arbitrary initial profile is chosen for  $\tilde{c}(r)$ , which varied monotonically from 0 in the reactants to 1 in the products. This profile is chosen after few preliminary simulations. The initial density values were obtained from the  $\tilde{c}$  profile.

The propagation of spherical flames during typical numerical calculations are shown in Fig. 1. The initial profiles are shown by dashed lines and the symbols in these figures indicate the spatial resolution of the grid and it shows that the flame brushes are well resolved. Figure 1a is the flame propagation when the effects of mean curvature are excluded from the mean scalar dissipation model (see Eq. 2) and Fig. 1b shows flame propagation when these effects are included using Eq. (3). The flame is propagating outwards from the centre and the last profile shown in symbols correspond to a simulation time of 1 ms. By comparing both figures it can be seen that the flame propagates faster when the curvature effects are included. This trend is observed for all the flames in Table 1.

Table 1: Attributes of the one-dimensional flames used for numerical simulation

Flame	$K$	$u'/s_L^0$	$\Lambda/\delta$	Da	Ka
F1	0.15	6.00	236.630	39.438	0.955
F2	1.00	12.0	42.593	3.549	6.369
F3	1.00	24.0	340.748	14.198	6.369

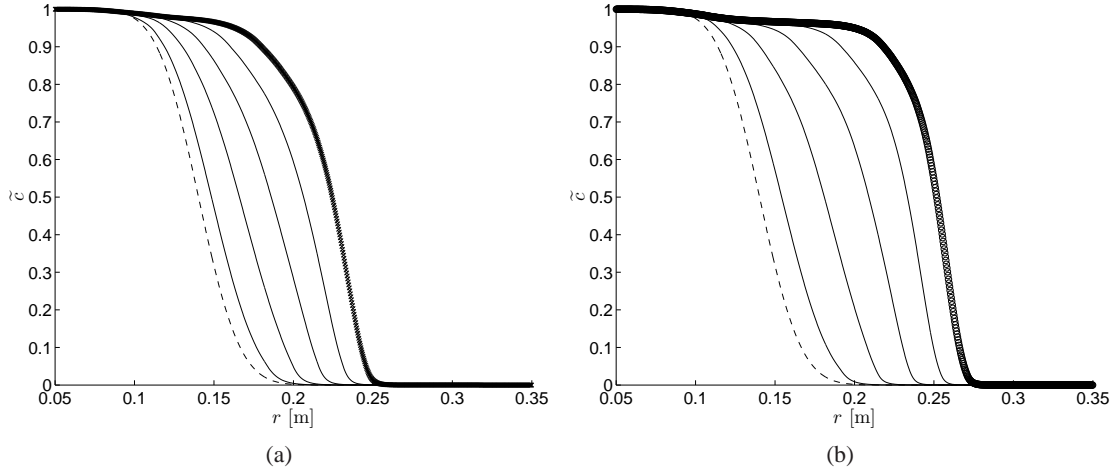


Figure 1: Propagation of flame F3: (a) without the effects of mean curvature. (b) with mean curvature effects. For both cases, the dashed lines show initial profiles, the time interval between consecutive profiles is 0.2 ms. The symbols are at 1 ms.

#### 4 Results and discussion

Fig. 2a shows the flame propagation speed  $dx(\tilde{c})/dt$ , for the flame F1 in Table 1, which is the sum of the displacement speed  $s_d$  and the flow velocity  $\tilde{u}_r$ . Here the iso-contours of  $\tilde{c} = 0.3, 0.5$  and  $0.7$  are plotted. This plot shows that once the initial transients die out all the iso-levels propagate at the same speed, attaining a constant value. This implies that even as the flame grows and the flame thickness increases, all the iso-contours will propagate outward at the same speed. This behaviour is observed for all the flames simulated and it is similar to the planar flame results reported by Kolla & Swaminathan [3].

In this work the turbulent flame speed  $s_T$  is defined as the displacement speed of the flame brush leading edge ( $\tilde{c} \simeq 0$ ). Comparison of the flame speed calculations using the two algebraic models for  $\tilde{\epsilon}_c$ , are shown in Fig. 2b. The results are again only shown for flame F3 since similar observations are made for the other flames tested. The flames calculated including the effects of mean curvature has a higher turbulent flame speed. The reason for this increase in flame speed can be seen from Eq. (3). For an outwardly propagating spherical flame the curvature term becomes  $\nabla \cdot n = 2/r_f$ . This increases the value of  $\tilde{\epsilon}_c$  for curved flames resulting in faster flame propagation. The second difference between the two  $\tilde{\epsilon}_c$  models is the efficiency factor  $\Gamma_K$ , which depends on the flame and turbulent properties since it is a function of length scale  $\Lambda/\delta_L^0$  and velocity scale  $u'/s_L^0$  [7]. It was found that the difference in flame speeds calculated from the two  $\tilde{\epsilon}_c$  models was the largest for flame F3, which had the largest  $\Gamma_K$  value. Whereas,  $\Gamma_K$  for flame F2 was small and the difference in flame speeds were smaller as well. This indicates that for the flames studied here  $\Gamma_K$  influence on the flame speed is higher in comparison to the curvature term effects. Further investigation is necessary to determine the applicability of the efficiency function for various spherical flames.

The normalised turbulent flame speeds for the flames in Table 1 using the two mean scalar dissipation

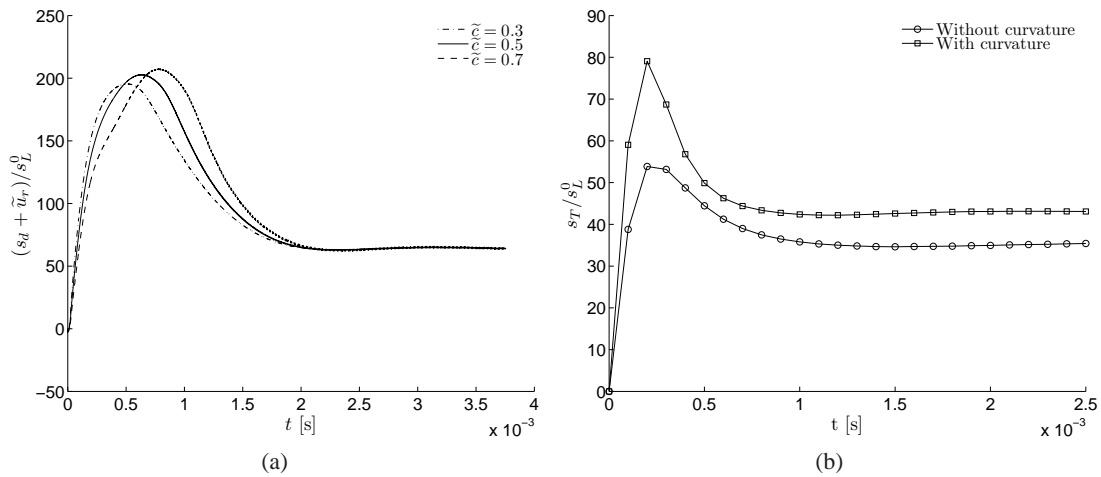


Figure 2: (a) Displacement speed for three iso-levels of  $\tilde{c}$  in flame F1 (b) comparison of displacement speeds with and without the effects of mean curvature for flame F3.

rate models are shown in Fig. 3a. The planar flame calculations for the same flames using the strained flamelet model is also plotted for comparison. As mentioned earlier, a higher flame speed is obtained for spherical flames when the curvature effects are included in the mean scalar dissipation rate model. It is interesting to note that the spherical flame speeds are considerably higher than the planar flame speeds. When the curvature effects are not included in the model for  $\tilde{c}_c$ , the reaction rate models of both the planar flames and spherical flames are identical. However, the spherical flame still propagates faster, which indicates that the increase in speed is purely due to geometric effects. This figure also shows that the difference in the flame speeds were large for the flame F3 compared with other flames. This is because this flame corresponds to a highly strained flame where the fluid dynamic stretch effects are amplified.

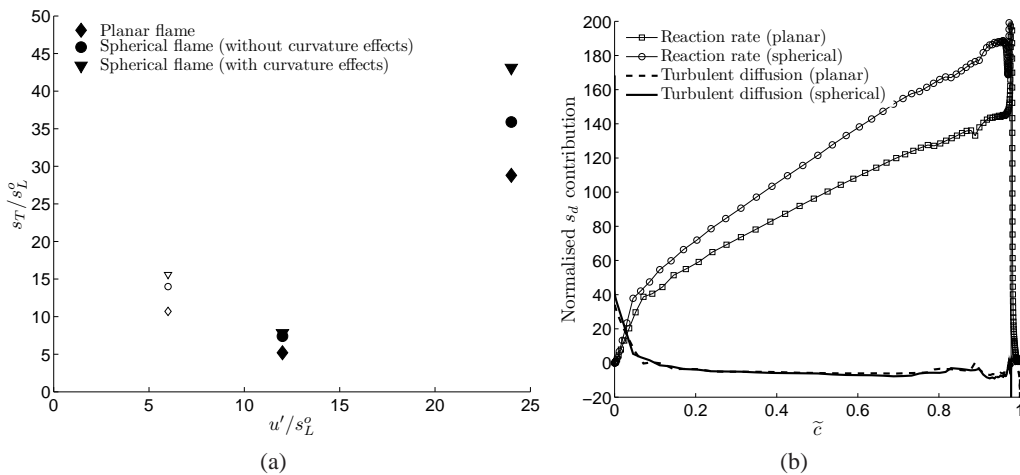


Figure 3: (a) Flame speed comparisons between spherical flames, with the inclusion and exclusion of curvature effects as well as planar flame speeds. Open symbols correspond to  $Ka = 0.955$  flame. (b) Contributions to the displacement speed for spherical flame F3 using the two  $\tilde{c}_c$  models. These speeds have been normalised with  $s_L^0$ .

According to the modelled transport equation for  $\tilde{c}$ , the displacement speed for a spherically propagating

flame is given by:

$$s_d = \bar{\omega} / \left( \bar{\rho} \left| \frac{\partial \tilde{c}}{\partial r} \right| \right) + \frac{1}{r^2} \frac{\partial}{\partial r} \left[ r^2 \left( \frac{\mu_t}{Sc_c} \frac{\partial \tilde{c}}{\partial r} \right) \right] / \left( \bar{\rho} \left| \frac{\partial \tilde{c}}{\partial r} \right| \right), \quad (6)$$

where the first term on the RHS is the reaction rate contribution to the displacement speed and the second term is the turbulent diffusion component. These contributions are plotted in Fig. 3b for spherically propagating flame F3, with the curvature effects included and excluded in the  $\tilde{c}_c$  model. It can be seen that the contribution due to turbulent diffusion is about the same order in both cases. However, the reaction rate contribution for the flame with curvature effects is considerably larger than that without curvature effects. This is again explained by the new terms in the  $\tilde{c}_c$  model. The same behaviour is observed for all the flame in Table 1.

## 5 Conclusion

Local strain and curvature effects of the flame will have an influence on the scalar gradients, which means that the scalar dissipation rate can be used as a parameter to capture these stretch effects. Spherically propagating turbulent premixed flames have been modelled using a strained flamelet model characterised using scalar dissipation rate. Two different algebraic models are used for the mean scalar dissipation rate, where the mean curvature effects were only included in one of the models. It is found that for all the flames simulated the flame propagation speed is higher when the curvature effects are included.

In these computations the governing equations were written in spherical coordinates where additional source terms appear. The physical effects of these extra terms appearing in the  $r$ -momentum equation and the turbulent kinetic energy equation will be investigated further and presented in the colloquium. The terms in these equations that contribute to the large increase in flame speed of spherical flames in comparison with planar flames will be addressed. In addition, the effect of changing the initial radius of the flame will be investigated further

## Selected references

- [1] Bray K.N.C. and Cant R.S. (1991). Some aspects of Kolmogorov's turbulence research in the field of combustion. Proc. R. Soc. Lond. A 434(1890):217-240
- [2] Jenkins K.W., Klein M., Chakraborty N. and Cant R.S. (2006). Effects of strain rate and curvature on the propagation of a spherical flame kernel in the thin-reaction-zones regime. Combust. Flame 145(1-2):415-434
- [3] Kolla H. and Swaminathan N. (2010). Strained flamelets for turbulent premixed flames, I: Formulation and planar flame results. Combust. Flame 157(5):943-954
- [4] Swaminathan N. and Bray K.N.C. (2005) Effect of dilatation on scalar dissipation in turbulent premixed flames. Combust. Flame 143(4):549-565
- [5] Kolla H., Rogerson J.W., Chakraborty N. and Swaminathan N. (2009). Scalar dissipation rate modeling and its validation. Combust. Sci. Technol. 181(3):518-535
- [6] Chakraborty N., Rogerson, J.W. and Swaminathan, N. (2010) The scalar gradient alignment statistics of flame kernels and its modelling implications for turbulent premixed combustion. Flow Turbul. Combust. 85(1):25-55
- [7] Meneveau C. and Poinso T. (1991) Stretching and quenching of flamelets in premixed turbulent combustion. Combust. Flame 86(4):311-332